Structure and formation mechanism of low-angle grain boundaries in chlorite

Toshihiro Kogure and Takashi Murakami

Mineralogical Institute, Graduate School of Science, University of Tokyo, Hongo, Tokyo 113, Japan

Abstract

The structure and formation mechanisms of low-angle grain boundaries (LAGB) in chlorite have been investigated using HRTEM to resolve each cation sheet in chlorite. The LAGB are abundant in two hydrothermally formed ferromagnesian chlorite specimens. Abundant LAGB, which are almost parallel to (001), divide chlorite grains into packets many tens of nanometers thick. They are initiated or terminated in a grain, indicating they are not formed as conjunctions of two grains growing independently. The boundaries consist of the (001) surface of a chlorite layer at one side and terminating chlorite layers at the other side, so that the grain boundary involves a series of misorientation of several degrees. Periodic rows of triangular regions surrounded by two (001) chlorite surfaces and one edge of the terminating layer along the boundary are formed along the LAGB. Distinct crystalline structure inside these triangles is not observed and brucite-like interlayers are absent at the (001) surfaces between triangular-shaped regions, indicating local compositional change along the boundaries. To explain the origin of this microstructure, a formation mechanism of these LAGB is proposed involving termination of the growth of one brucite-like interlayer on a (001) TOT layer surface during layer-by-layer growth.

Introduction

Chlorite is a common and important layer silicate formed under a wide range of conditions. It is found in low-to-medium grade metamorphic rocks, pegmatites, fissure vein deposits, and in altered igneous rocks as a secondary mineral that replaces primary ferromagnesian minerals like biotite (Bailey 1988). Its well-known crystal structure consists of a TOT (tetrahedral-octahedral-tetrahedral) talc-like layer and a brucite-like interlayer. There has been considerable interest in the chlorite formation mechanism during metamorphism and alteration. Precipitation from solution and direct, solid-state transformation from original minerals have been suggested. Observations by many workers suggest that chlorite forms by both mechanisms, depending on the environment in which chlorite growth takes place (e.g., Veblen and Ferry 1983; Olives-Baños and Amouric 1984; Eggleton and Banfield 1985; Ahn and Peacor 1985; Yau et al. 1988; Baronnet and Kang 1989). High-resolution transmission electron microscopy (HRTEM) is a powerful method that enables us to investigate chlorite microstructures, distinguishing each cation sheet in a chlorite unit cell (Bons and Schryvers 1989; Banfield et al. 1994; Banfield and Bailey 1996). This study reports numerous low-angle grain boundaries (hereafter abbreviated as LAGB) in some chlorite specimens through HRTEM and discusses their formation mechanism. The results pertain to the understanding of chlorite formation, as well as the stability, diffusion, and mechanical properties, by revealing the atomic structure of the grain boundaries in this mineral.

Experimental method

Two chlorite specimens containing abundant LAGB were studied in detail. One specimen is chlorite from a hydrothermally altered granite from Gogoshima, Ehime prefecture, Japan. Chlorite crystals are 1–2 mm in size and pale green under plane polarized light in petrographic thin sections. These chlorite crystals obviously replaced original biotite in granite because biotite is abundant in less altered granite from the same locality. Peak positions in the X-ray diffraction pattern indicate ferromagnesian chlorite with no interstratification of biotite layers (Reynolds 1988). Furthermore, no biotite layers were found in preliminary TEM observations, suggesting this replacement was not direct (solid-to-solid) transformation from biotite to chlorite, as reported by many authors (Veblen and Ferry 1983; Olives-Baños and Amouric 1984; Eggleton and Banfield 1985; Kogure 1996). The second specimen is an aggregate of small ferromagnesian chlorite flakes (sub-millimeter in size) in a chlorite-quartz-chalcopyrite vein from Osaruzawa mine, Akita prefecture, Japan (Shirozu 1963). Chlorite grains were extracted, ground, and mounted in an epoxy resin, applying pressure so that the (001) planes of the chlorite fragments were oriented (Ferrow and Roots 1989). Epoxy-chlorite slabs were sliced perpendicular to the (001) planes, polished mechanically, and thinned to electron transparency by argon ion-milling. Finally, samples were carbon coated before they were examined by TEM. HRTEM observation was performed at 200kV using a JEOL JEM-2010 electron microscope (Cs = 0.5 mm) with a LaB_6 filament. The point resolution is ~0.2 nm, which allows each cat-
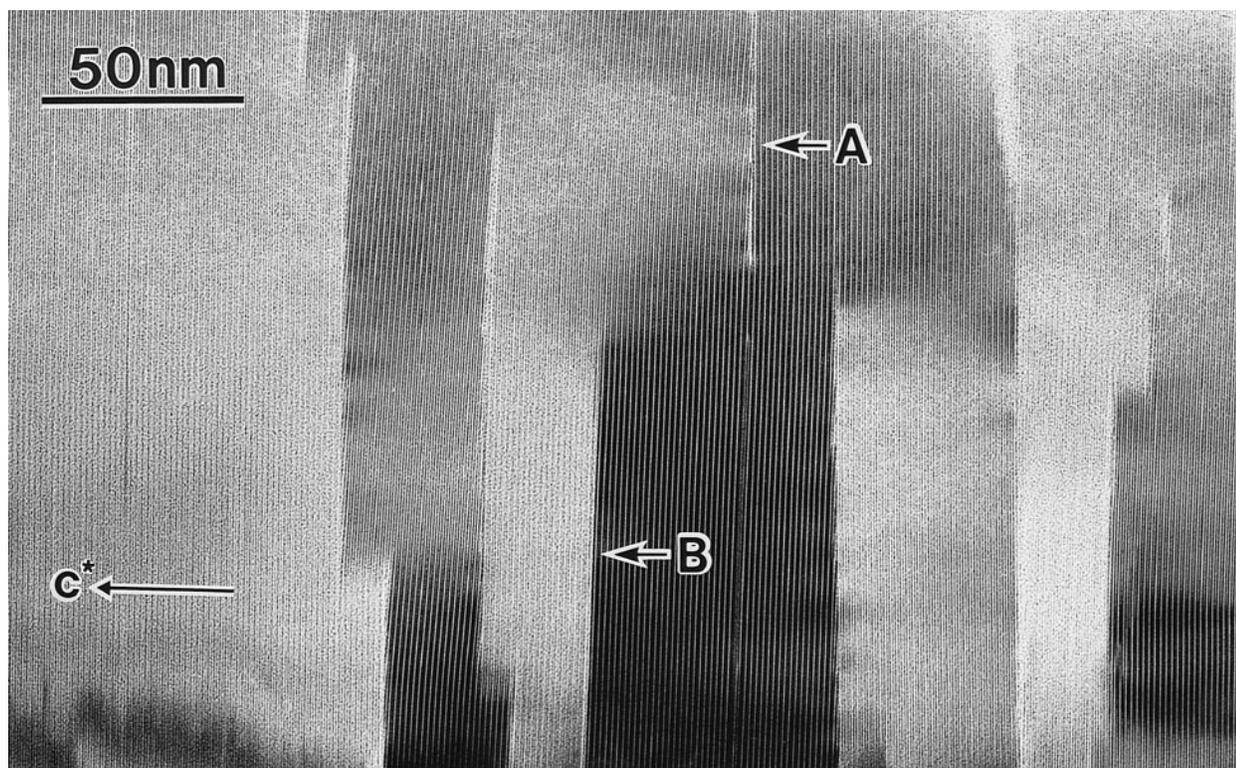
FIGURE 1. HRTEM image of chlorite from altered granite observed approximately along ⟨010⟩. Planar defects are observed commonly as indicated by the arrows A and B. At defect A the lattice fringes are inclined to each other whereas at defect B (001) fringes are almost parallel on both sides of the defect. Some planar defects are initiated or terminated in the grain.

ion sheet in the chlorite structure to be distinguished when the sample is observed along [*hk*0] directions. As described by Bons and Schryvers (1989), it is difficult to distinguish the beam direction among [100], [110], and [1$\bar{1}$0] (they are equivalent in the pseudohexagonal cell of chlorite) during practical TEM observation if chlorite stacking is semi-random. However, observations along [100], [110], and [1$\bar{1}$0] are equally useful for the analysis presented in this paper. These directions are indicated as ⟨100⟩ after Bons and Schryvers (1989). Similarly [010], [310], and [$\bar{3}$10] are indicated as ⟨010⟩.

RESULTS AND INTERPRETATION

Figure 1 shows a typical lattice image of chlorite from altered granite observed approximately from the ⟨010⟩ direction. Planar defects commonly divide the chlorite grain into layer packets many tens of nanometers wide. It appears that there are two kinds of planar defects. One type is immediately recognized as LAGB from the image (indicated by A in Fig. 1), where the (001) planes on either side are not parallel but inclined by several degrees to each other. The other type of planar defect has almost parallel (001) planes at both sides but the boundary is distinguishable by the difference of diffraction contrast between each side (B in Fig. 1). Selected-area electron diffraction (SAED) patterns from areas that contain similar defects to those labeled "A" and "B" in Figure 1 are

shown in Figures 2a and 2b, respectively. These SAED patterns indicate that the (001) planes, or *c** axes, are inclined to each other. In the first case, *c** is rotated in the plane of the figure and in the second, *c** is rotated normal to the plane of the figure, suggesting that both types of defects are similar and involve small angular misorientations between each side (LAGB). To investigate these microstructures, the LAGB should be observed parallel to the axis common to the chlorite on either side of the grain boundary. From many observations of SAED patterns the common crystal axis in both sides of the boundaries is generally either ⟨100⟩ or ⟨010⟩, as indicated in Figure 2.

Figure 3 illustrates LAGB in chlorite from a chlorite-quartz-chalcopyrite vein observed along ⟨010⟩. In this specimen we observe a similar high density of boundaries that are sometimes initiated (indicated by the arrow in Fig. 3) or terminated within a grain. The contrast along the boundary indicated by the arrowheads in Figure 3 is probably due to strain.

Figure 4 shows ⟨100⟩ and ⟨010⟩ LAGB high-resolution images that resolve the tetrahedral and octahedral sheets and brucite-like interlayers. Observed from [*hk*0] directions, the trioctahedral brucite-like interlayer is imaged as continuous black line contrast. This has previously been reported by Bons and Schryvers (1989), Banfield et al. (1994), and others, and is confirmed by our multislice
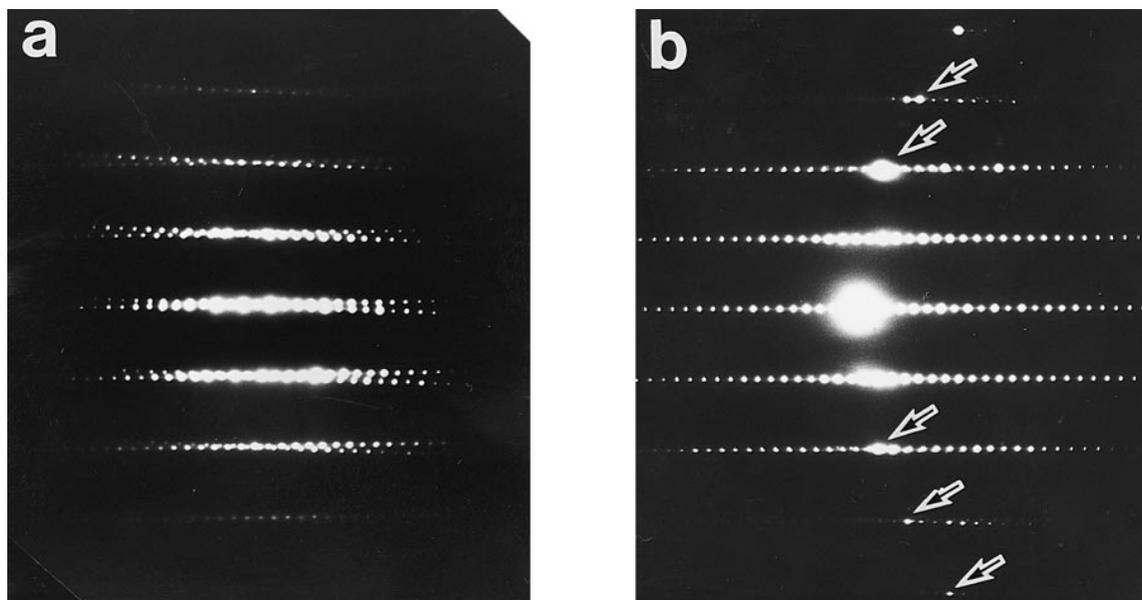
FIGURE 2. SAED pattern from areas that contains planar defects similar to (**a**) defect A or (**b**) defect B in Figure 1. The beam direction is $\langle 010 \rangle$. Both c^* axes are on the observing plane in **a** whereas one is on the plane and the other is not, but forming an arc of zero-order Laue zone (ZOLZ) as indicated by arrows in **b**.
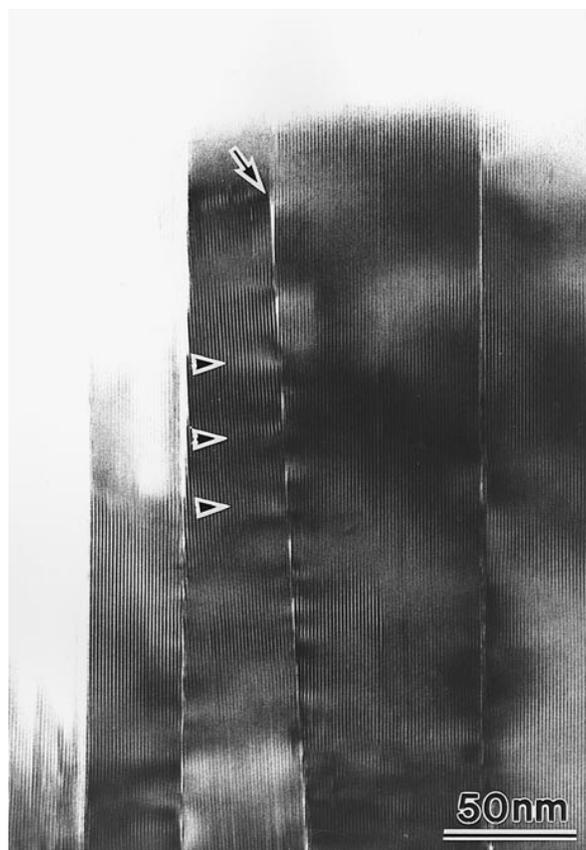

FIGURE 3. HRTEM image of chlorite in a chlorite-quartz-chalcopyrite vein. The beam direction is $\langle 010 \rangle$. The arrow indicates the point where a LAGB is initiated.

simulations for images recorded from thin specimens at close to Scherzer defocus. The TOT layer has contrast involving three fine continuous black lines corresponding to the three sheets when observed from [$hk0$]. The tetrahedral sheets are imaged as spotty lines when observed from $\langle 100 \rangle$, as shown in Figure 4a. The LAGB consist of the (001) surface of a layer at one side and terminating layers at the other side, inclined by about 3 to 5° from the opposite (001) plane. The terminating layers and the opposite continuous layers are bent slightly at the LAGB (viewing the photographs at a low angle along the boundaries makes the details easy to see). Along the LAGB, a row of triangular regions (they actually have the shape of a triangular prism extending to the common axis) is generated by a set of two (001) surfaces and one terminating edge of a chlorite layer.

The contrast inside the triangle suggests that it is amorphous. The question is whether this represents the original structure of the material or whether this is an artifact. Generally, silicates containing water molecules or hydroxyls are beam sensitive (Iijima and Zhu 1982). Chlorite is also easily damaged by beam radiation and moreover grain boundaries are weaker than normal regions (Veblen 1983). Thus, the amorphous contrast in the triangles may be formed during observation by beam damage of terminating layers. Figure 5a shows a high-resolution image of a LAGB from $\langle 100 \rangle$ and Figure 5b shows the same area taken after about 20 s with beam intensity of about a few amperes per square centimeters on the specimen (the total electron dose in Fig. 5b is estimated to be many times more than that in Fig. 5a). Damage in chlorite begins at the (001) surface of the chlorite layers
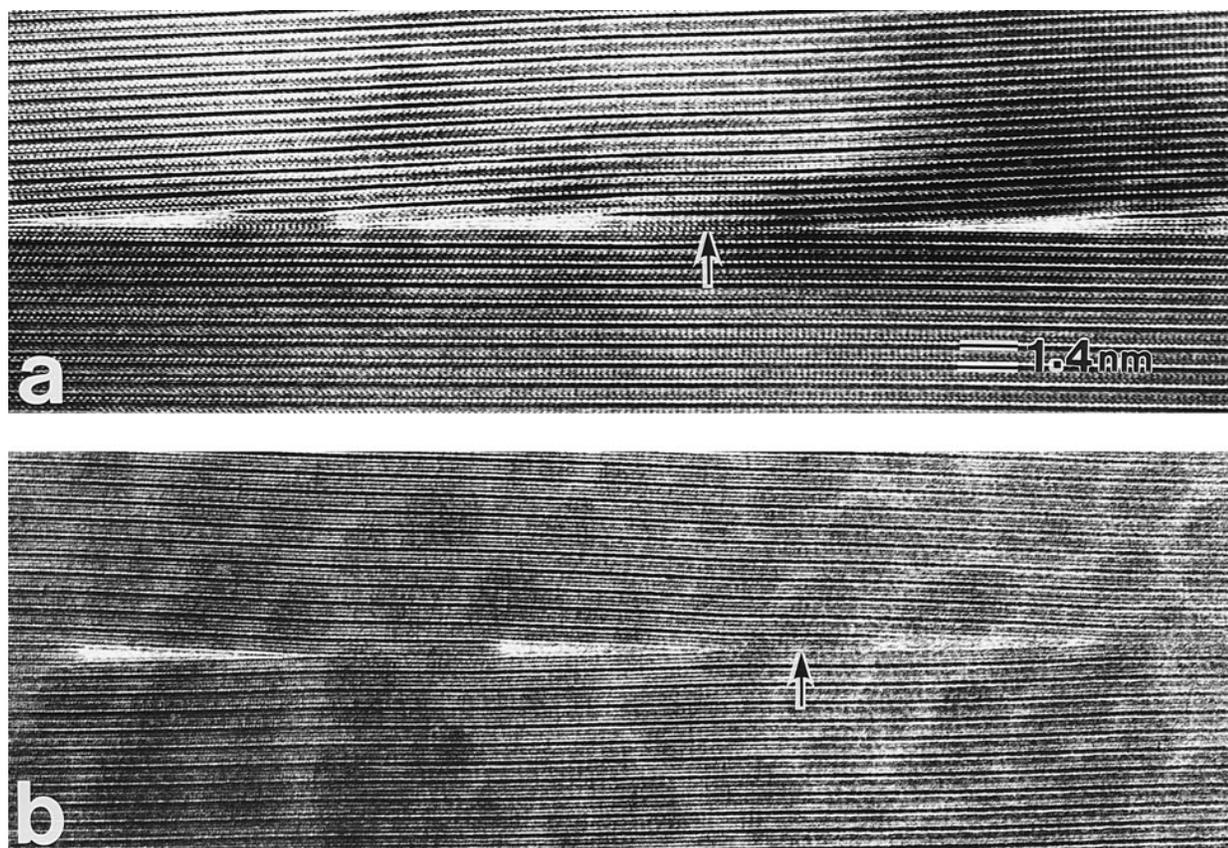
FIGURE 4. (**a**) Magnified image of a LAGB whose common axis is ⟨100⟩. The terminating chlorite layers are bent in contact with the layer on the other side of the boundary (view the photograph at a low angle along the boundary). (**b**) Magnified image of another LAGB whose common axis is ⟨010⟩. Three cation sheets in a TOT layer correspond to three fine black lines and the brucite-like layer has the contrast of the boldest black line. It is clearly indicated that two TOT layers are in contact without a brucite-like sheet at the area indicated by the arrow in both figures.

on both sides of the LAGB, not at the terminating front of the layer. This result suggests it is unlikely that triangular region was filled originally with crystalline material that was vitrified by beam radiation.

An important feature around the LAGB in HRTEM images in Figure 4 is the absence of brucite-like interlayer at the boundary. Contrast details indicate the boundary consists of two TOT layers between two triangles as indicated by the arrows in Figure 4a and 4b, which implies that these LAGB are not arrays of simple edge dislocations and that the local chemical composition is different from normal chlorite. Considering the high density of the LAGB as shown in Figure 1, octahedral cations in the chlorite grain may be slightly deficient.

Finally, Figure 6 shows a HRTEM image of one isolated triangular region accompanying the termination of one chlorite layer. One chlorite layer and one brucite-like interlayer (one TOT layer and two brucite-like interlayers totally) are missing at the upper part of the triangle. The brucite-like interlayer indicated by the arrowhead disappears first as these layers approach the triangle from the top of the figure. On the other hand, the contrast near the bottom of the figure, though it changes due to increased specimen thickness as compared with that in the top of the figure, indicates that no brucite-like interlayer is missing, which suggests one brucite-like interlayer is formed or recovered at the closing point of the triangle. These structures at the top and bottom of the triangle in Figure 6 may correspond to the trigger and terminating points of LAGB, respectively, as discussed in the following section.

DISCUSSION

The LAGB described above cannot be regarded as simple interfaces between two adjacent chlorite grains because they are usually initiated or terminated in a grain. The chlorite layers on both sides may have formed by unidirectional growth (e.g., from the bottom to the top in Figs. 4a and 4b) so that the terminating layers are formed later than those parallel to the boundary. The proposed mechanism for formation of these LAGB (Fig. 7) assumes that a TOT layer and a brucite-like interlayer grow together. During layer-by-layer growth on the (001) surface of chlorite from solution, a brucite-like sheet may
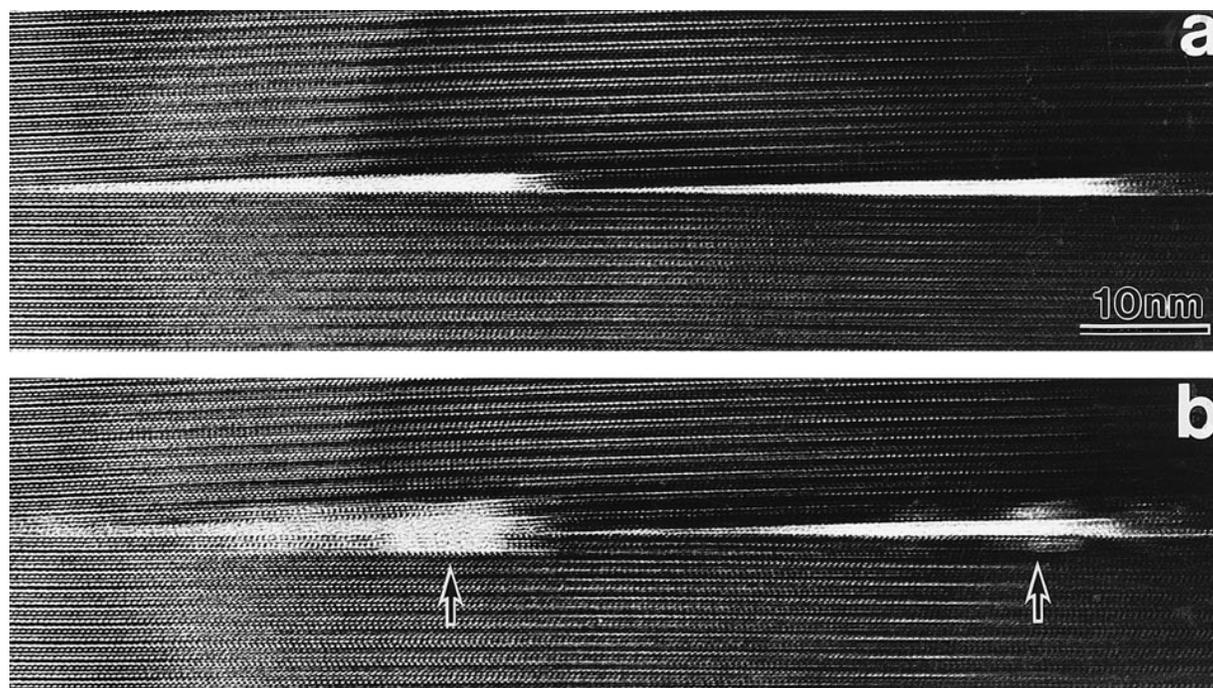
FIGURE 5. (**a**) Magnified image of a LAGB observed from ⟨100⟩. (**b**) Image of the same area after beam radiation for about 20 s. The chlorite layers on both sides of the boundary are starting to be vitrified as indicated by arrows. The structure in the chlorite layer can be distinguished in the thinner area (left side).

stop growing for some reason (X in Fig. 7a), for example due to a local deficiency of the elements required to form the brucite-like layer, but the TOT layer under it could continue to grow. In this model the formation of LAGB is triggered when a brucite-like sheet ceases to grow and effectively terminates. (An example of a brucite-like sheet, which has stopped growing, is indicated by an arrow in Fig. 6.) The next chlorite layer reaches the point where the previous brucite-like sheet stopped and bends downward until it makes contact with the surface of the previous TOT layer as observed in Figure 4 (Fig. 7b). This contact, which consists of two TOT layers, has no interlayer charge and this chlorite layer may change its speed of growth. If the speed is decreased, this chlorite layer is passed by the next layer. The next chlorite layer also bends downward after it exceeds the terminating point of the previous chlorite layer and contacts the surface of the previous TOT layer (Fig. 7c). If brucite-like sheets form again at this contact, the normal growth is recovered, leaving a triangular region as shown in the bottom of the triangle in Figure 6. However, the contact of two TOT layers without an interlayer decreases its growth speed again. If this occurs repeatedly, a LAGB is formed (Fig. 7d). If the chlorite layer grows with a unit of a brucite-like interlayer and a TOT layer together (reversed order) or grows with each unit separately, we can obtain the same LAGB structure if we assume that the brucite-like interlayer can only grow onto a TOT layer and the TOT layer can grow without the brucite-like in-

terlayer below it. This difference between these two units in a chlorite layer may be attributed to the opposite layer charge of the two units, although the local compositions of these two units in chlorite layers around LAGB may be changed so that they have a lower charge. The surface of the TOT layer (negatively charged) may be easily neutralized by the positive ions (for example, protons) in solution.

Finally we discuss whether such boundaries are common in chlorite. Veblen (1983) reported that LAGB were common in metamorphic chlorite. Although the reported image shows similar features to those in our work, the boundary was too damaged to allow us to determine whether it is identical. Yau et al. (1988) also presented an image of a grain boundary in chlorite from geothermally altered shales. However the resolution of the TEM image is not sufficient for detailed discussion. Bons et al. (1990) reported a HRTEM image of the LAGB in slates with a sufficient resolution to identify cation sheets in chlorite. No triangular regions or missing brucite-like interlayer at the boundary were seen, suggesting a different origin for the LAGB from that in this work. Parseval et al. (1994) presented a low-magnification TEM micrograph of chlorite formed by hydrothermal alteration of mica (a similar origin to one of the specimens in our work). Although the magnification is too low to see lattice fringes, the chlorite grain is divided by planar defects into packets as the image in Figure 1. These planar de-
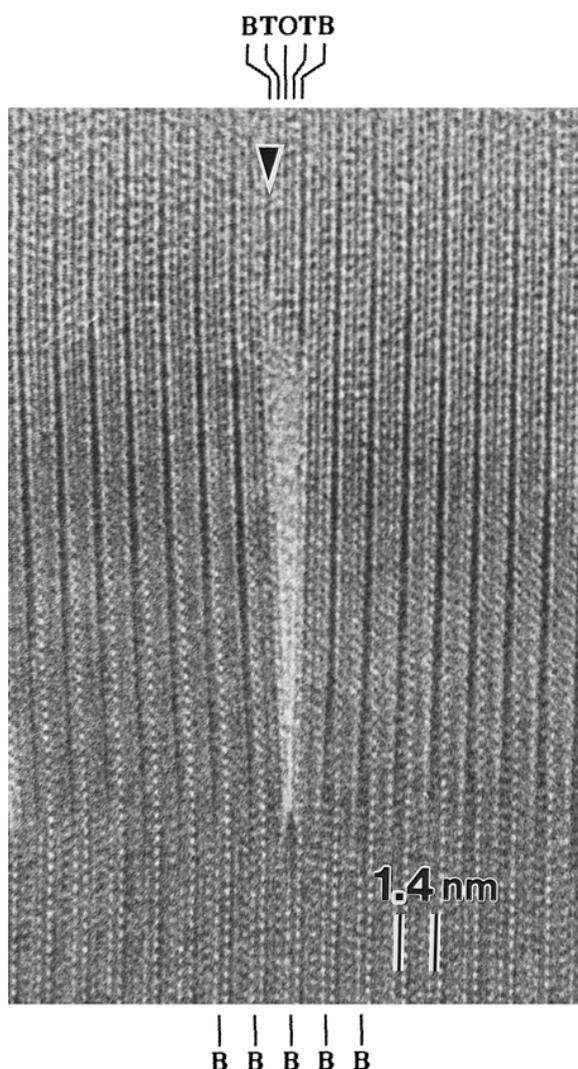
BTOTB

FIGURE 6. A single triangular region observed from ⟨100⟩. B, T, and O indicate the position of brucite-like interlayer, tetrahedral and octahedral sheet in TOT layer, respectively. Note one TOT layer and two brucite-like sheets are missing at the top of the triangle. The arrowhead indicates the brucite-like sheet which is first terminated compared with another brucite-like sheet and the TOT layer. One the other hand, no brucite-like interlayer is missing where the triangle is closed at the bottom of the figure.

fects may be LAGB structures similar to those described here.

In our investigation LAGB have not been observed in chlorite that is considered formed by direct transformation from biotite (this chlorite is characterized by frequent interstratification of biotite and chlorite layers, Veblen and Ferry 1983). Formation of these boundaries during layer-by-layer growth on the free crystal surface, as described above, is consistent with crystallization from solution. On the other hand, not all chlorite formed from solution contains such LAGB: Only a few LAGB are found in some of our other specimens, which apparently
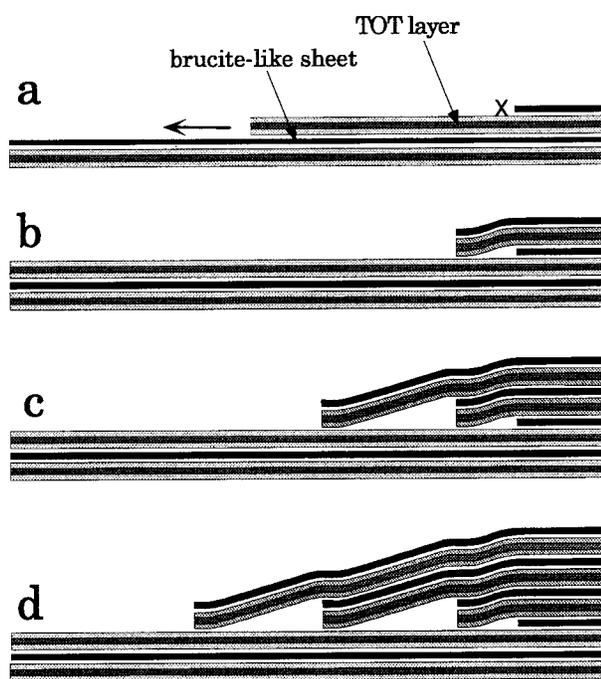

FIGURE 7. Schematic illustration of the formation mechanism of LAGB (see text for details).

also formed from solution. Perhaps the key may be whether or not brucite-like interlayers form stably in the growing environment.

REFERENCES CITED

Ahn, J.H. and Peacor, D.R. (1985) Transmission electron microscopic study of diagenetic chlorite in Gulf Coast argillaceous sediments. Clays and Clay Minerals, 33, 228–236.

Bailey, S.W. (1988) Chlorites: Structure and crystal chemistry. In Mineralogical Society of America Reviews in Mineralogy, 19, 347–403.

Banfield, J.F. and Bailey, S.W. (1996) Formation of regularly interstratified serpentine-chlorite minerals by tetrahedral inversion in long-period serpentine polytipes. American Mineralogist, 81, 79–91.

Banfield, J.F., Bailey, S.W., and Barker, W.W. (1994) Polysomatism, polytypism, defect structures, and reaction mechanisms in regularly and randomly interstratified serpentine and chlorite. Contribution to Mineralogy and Petrology, 117, 137–150.

Baronnet, A. and Kang, Z.C. (1989) About the origin of mica polytypes. Phase Transitions, 16/17, 477–493.

Bons, A.J. and Schryvers, D. (1989) High-resolution electron microscopy of stacking irregularities in chlorites from the central Pyrenees. American Mineralogist, 74, 1113–1123.

Bons, A.J., Drury, M.R., Schryvers, D., and Zwart, H.J. (1990) The nature of grain boundaries in slates. Physics and Chemistry of Minerals, 17, 402–408.

Eggleton, R.A. and Banfield, J.F. (1985) The alteration of granitic biotite to chlorite. American Mineralogist, 70, 902–910.

Ferrow, E.A. and Roots, M. (1989) A preparation technique for TEM specimens; applications to synthtic Mg-chlorite. European Journal of Mineralogy, 1, 815–819.

Iijima, S. and Zhu, J. (1982) Electron microscopy of a muscovite-biotite interface. American Mineralogist, 67, 1195–1205.

Kogure, T, (1996) Investigation of alteration processes of biotite by high resolution electron microscopy. Ph.D. thesis, University of Tokyo, Japan.

Olives-Baños, J. and Amouric, M. (1984) Biotite chloritization by interlayer brucitization as seen by HRTEM. American Mineralogist, 69, 869–871.

Parseval, P.D., Amouric, M., Baronnet, A., Fortune, J., Moine, B., and Ferret, J. (1994) HRTEM study of the chloritization of mica in the talc-chlorite deposit at Trimous (Pyrenees, France). European Journal of Mineralogy, 6, 123–132.

Reynolds, R.C., Jr. (1988) Mixed layer chlorite minerals. In Mineralogical Society of America Reviews in Mineralogy, 19, 601–629.

Shirozu, H. (1963) Structural changes of some chlorites by grinding. Mineralogical Journal, 4, 1–11.

Veblen, D.R. (1983) Microstructures and mixed layering in intergrown wonesite, chlorite, talc, biotite, and kaolinite. American Mineralogist, 68, 566–580.

Veblen, D.R. and Ferry, J.M. (1983) A TEM study of the biotite–chlorite reaction and comparison with petrologic observations. American Mineralogist, 68, 1160–1168.

Yau, Y.C., Peacor, D.R., Beane, R.E., Essene, E.J., and McDowell, S.D. (1988) Microstructures, formation mechanisms, and depth-zoning of phyllosilicates in geothermally altered shales, Salton Sea, California. Clays and Clay Minerals, 36, 1–10.